Semiconductor nanowire photoluminescence: spatial/polarization averaged coupling into leaky modes

R. Paniagua-Domínguez[a], G. Grzela[b], J. Gómez Rivas[b,c], and J. A. Sánchez-Gil[a]

[a]Instituto de Estructura de la Materia (IEM-CSIC), Consejo Superior de Investigaciones Científicas, Serrano 121, E-28006 Madrid, Spain;
[b]FOM Institute for Atomic and Molecular Physics (AMOLF), c/o Philips Research, High-Tech Campus 4, 5656 AE Eindhoven, The Netherlands;
[c]COBRA Research Institute, Eindhoven University of Technology, P.O. Box 513, 5600 MB Eindhoven, The Netherlands

ABSTRACT

Photoluminescence from finite semiconductor nanowires is theoretically investigated. We show experimentally the directional emission of polarized light from single InP nanowires through Fourier microphotoluminescence, thus demonstrating semiconductor nanowires behave as efficient optical nanoantennas. Numerical calculations for finite nanowires confirm such enhanced and directional emission. We anticipate the relevance of these results for the development of nanowire photon sources with optimized efficiency and controlled emission.

Keywords: semiconductor NWs, photoluminescence, nanophotonics

1. INTRODUCTION

Photoluminescence from semiconductor nanowires (NWs) is attracting a great deal of attention in recent years.[1–3] This stems from the variety of applications in Nanophotonics where the optical properties (scattering, absorption and emission) of NWs play a leading role:[1–14] namely, light-emitting devices, single-photon sources, photodetectors, solar cells, . . .

Particularly relevant to NW photoluminescence are the electromagnetic modes supported by the nanowire,[15] which determine the allowed emission channels through their corresponding local density of states, and also the emission characteristics through their outcoupling into propagating waves.[16–19] Indeed, it has been shown theoretically[19] and confirmed experimentally,[14] that the semiconductor nanowire thus plays the role of a photoluminescent nanoantenna, either through leaky[14] or guided[14] modes. However, only single dipole emission has been considered from the theoretical standpoint to explain the NW photoluminescence antenna emission,[14] whereas in truth photoluminescence occurs uniformly throughout the NW (unless selected by the exciting beam), with random polarization. In this work, we will take into account in the theoretical calculations spatial and orientation averaging of the emission, based on the same configuration as that used in 14, to give support to the NW antenna emission mediated by leaky mode coupling.

2. DISPERSION RELATION

First, let us examine the modes supported by an infinite InP NW. We will consider from now on the same configuration as that used in 14: an InP NW with radius $R = 50$ nm, length $L = 3\,\mu$m, standing vertically on an InP substrate, emitting at $\lambda = 880$ nm ($n_{\text{InP}} = 3.42$, cf. Ref. 20). We thus calculate the dispersion relation,[15] for fixed wavelength at 880 nm with varying radius R. The results are shown in Fig. 1. Two modes are found: The no-cutoff HE_{11} guided mode and the leaky mode TM_{01}. The former (HE_{11}) mode lies on top of the light line and is very weakly guided. Its electric field amplitude inside the NW (shown in Fig. 1(b)) is indeed small. The leaky mode TM_{01}, by contrast, exhibits a strong electric field component along the NW axis inside the NW, with a maximum at the center. Since the electric field amplitudes are connected to the electromagnetic mode local density of states (LDOS), the leaky mode it is thus expected to play a leading role in the resulting photoluminescence.[14]
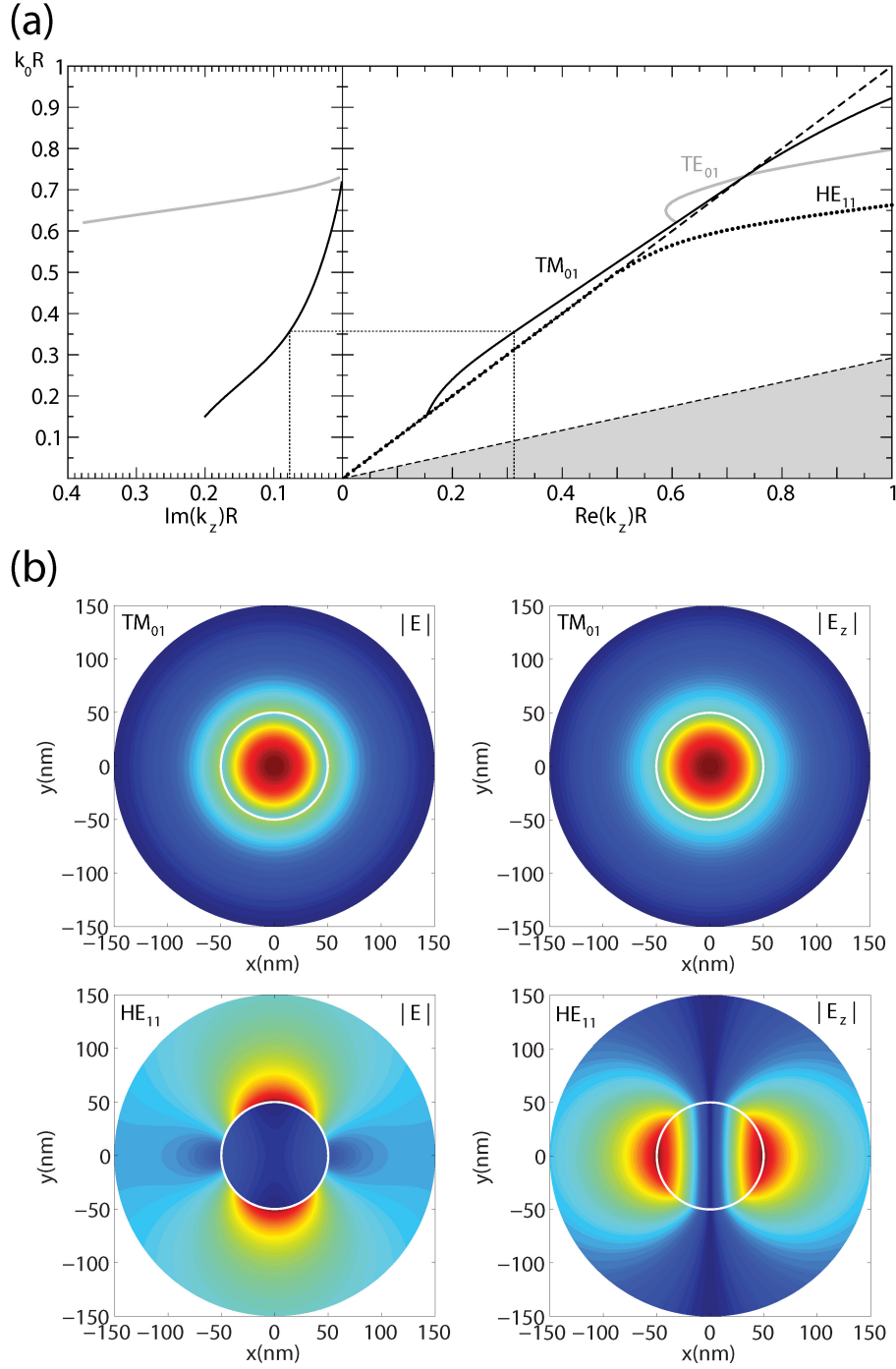

Figure 1. (a) Right panel: Dispersion relations of the leaky mode TM_{01} (solid curve) and the weakly guided HE_{11} mode (dotted curve) supported by an infinite InP cylinder with varying radius R at fixed $\lambda = 880$ nm, $n_{InP} \simeq 3.42$. The dashed line represents the light line. The TE_{01} mode (light curve) is also included for the sake of completeness. Left panel: Imaginary part of the wavevector of the leaky modes, TM_{01} (solid curve, only for $K_0 R < 0.72$) and TE_{01} (light curve) (b) Cross-sectional contour maps of the modulus of the total electric field (left column) and its z- component (right column), inside and outside the cylinder (denoted by a white circle) of the modes supported at fixed $\lambda = 880$ nm and $R = 50$ nm: the leaky TM_{01} mode (top) and the weakly guided HE_{11} mode (bottom).
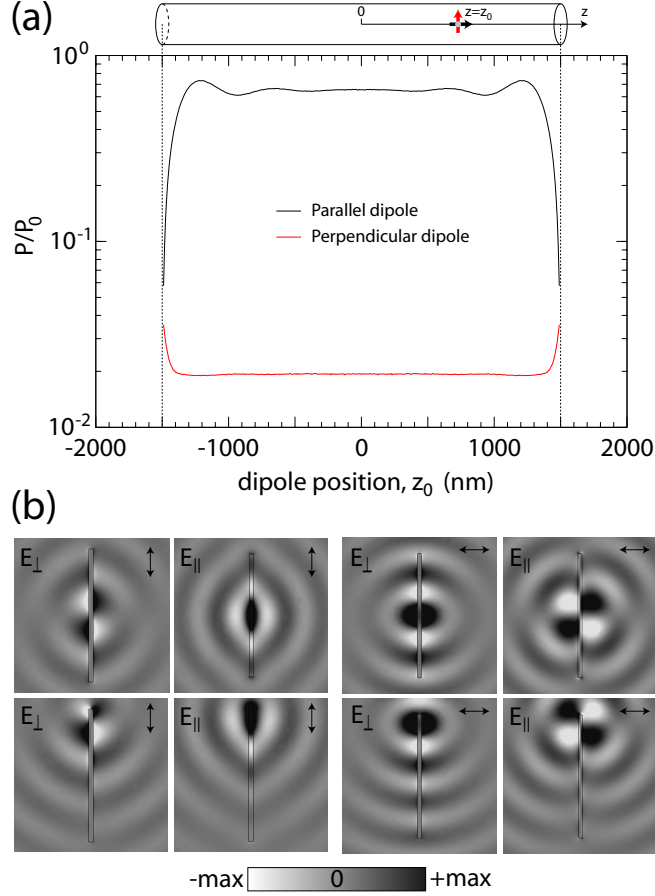
Figure 2. (a) Normalized radiated power P/P_0 as a function of (parallel and perpendicular) dipole position z_0 at the NW axis for a finite ($L = 3\,\mu\mathrm{m}$) InP nanowire with $R = 50$ nm at $\lambda = 880$ nm. (b) Contour maps of the of the parallel $E_{\parallel}$ and perpendicular $E_{\perp}$ components of the electric field in the vicinity of the NW as in (a), for emitting dipoles with parallel (left) and perpendicular (right) polarization that are located on the NW axis either at the NW center (top) or at $d = 200$ nm from the NW edge (bottom).

3. LEAKY-MODE COUPLING IN FINITE NANOWIRES

Next, let us study the photoluminescence of a finite InP NW with $L = 3.13\,\mu\mathrm{m}$, as in Ref. 14. We focus on the optical emission process, which is modeled by the emission of a point dipole located inside the NW. This is done through FEM numerical simulations through COMSOL, as detailed in the Appendix. We assume that the dipole is located along the NW axis, and calculate the total power flow as a function of dipole position along the NW axis, as shown in Fig. 2(a). The emission is nearly constant throughout the NW, except at distances close to the NW edges. The electric field pattern inside the NW for two different dipole positions is also plotted, see Fig. 2(b). Such electric field pattern matches that of the TM_{01} leaky mode shown above in Fig. 1(b), confirming the predominant coupling of the parallel dipole to such mode (coupling from the perpendicular dipole is however inhibited due to the LDOS symmetry). Actually, the slow oscillations of the power flow when the parallel dipole is located close to the NW edges agree as well with this argument, for their period and decay length coincide with the mode wavelength and leakage decay length, inversely related to the real and imaginary parts of the mode wavevector (see Fig. 1(a)), respectively.

However, NW photoluminescence expectedly occurs uniformly throughout the NW, with transition dipole contributions that are randomly oriented. To properly characterize such process, we calculate the angular distribution of PL light emitted from a set of dipoles with three different orientations (one perpendicular and two parallel to the NW axis) evenly distributed throughout the NW axis (off-axis emission is neglected); all
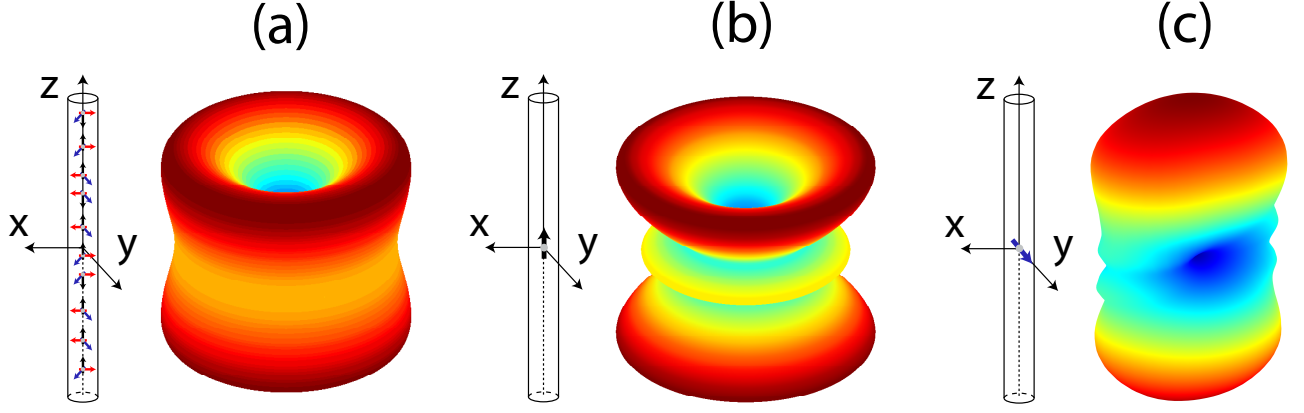
Figure 3. (a) Total far-field intensities of the light emitted by an ensemble of 3×300 dipoles with three different orientations (one parallel and two perpendicular to the NW axis) evenly distributed throughout the NW axis for a finite ($L = 3\,\mu$m) InP NW with $R = 50$ nm at $\lambda = 880$ nm. (b,c) Total far-field intensities of the light emitted by two dipoles located at the NW center, polarized either parallel (b) or perpendicular (c) to the NW axis.
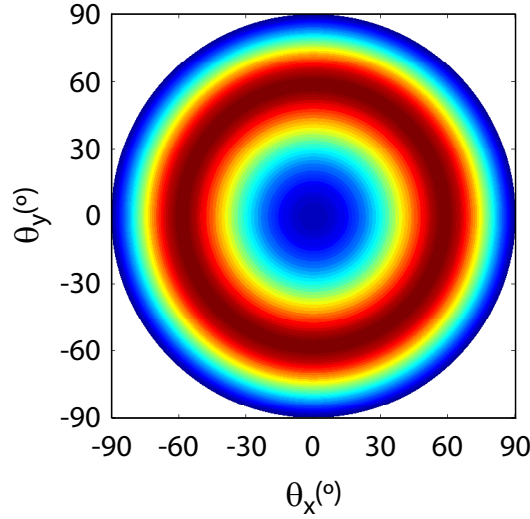

Figure 4. Unpolarized directional emission, angularly projected as a Fourier microscopy image,[14] from an ensemble of 3×300 dipoles with three different orientations (one parallel and two perpendicular to the NW axis) evenly distributed throughout the InP NW axis ($L = 3\,\mu$m and $R = 50$ nm). The dipoles radiate at a wavelength of $\lambda = 880$ nm.

contributions are incoherently added. The results are shown in Fig. 3(a); for the sake of comparison, the contributions from a parallel and a perpendicular dipole located at the NW center are included separately in Fig. 3(b,c). It is thus evident from Fig. 3 that the parallel dipole coupling into the TM_{01} leaky mode, exhibiting a *diabolo*-like shape, is the dominant contribution upon spatial/orientation averaging, resulting only in a slight broadening of the equatorial lobe.

Furthermore, to confirm that this argument in turn explains the PL measurements reported in Ref.[14] (Fig. 2), let us plot in Fig. 4 the total, unpolarized far-field intensities of the light emitted by the ensemble average shown in Fig. 3(a), now projected in the form of Fourier-microscopy images. The expected doughnut shape with predominant radial polarization is obtained, revealing a good agreement with the Fourier-microscope measurements.

4. CONCLUDING REMARKS

In conclusion, we have shown through finite element simulations of a dipole source embedded in an InP nanowire, that the directional emission is ruled by the TM_{01} leaky mode supported by the nanowires. To yield further evidence that this is the case for experimental nanowire photoluminescence, for which randomly polarized emission is expected from throughout the nanowire, numerical calculations are carried out that average incoherently contributions from dipoles with three different orientations evenly distributed throughout the nanowire axis. The resulting angular distribution of emitted light is qualitatively and quantitatively governed by the most relevant contribution, stemming from parallel dipole coupling into the TM_{01} leaky mode. The nanowire thus playing the role of a photoluminescent nanoantenna,[14] which can be exploited to tune the intensity and direction of emission in a variety of applications in Nanophotonics.

APPENDIX A. COMSOL NUMERICAL SIMULATIONS

Finite-element-method-based numerical simulations were performed using commercial software COMSOL Multyphysics v4.3. The simulated space consists of a circular cylinder of length L and diameter $2R$, representing the nanowire, and two concentric spheres of radii $0.7L$ and $1.1L$, respectively, with their centers coinciding with that of the cylinder. In the outer sphere an additional spherical layer of thickness $0.2L$ was defined. Aside from the cylinder, this geometry divides the simulation space into three concentric spherical subdomains. They were all set to be air ($n_{Air} = 1$). The outer spherical layer was define as a perfectly matched layer (PML) to absorb all the outgoing radiation. In the case of the NW lying vertically on a substrate, the spherical domains and the outer shell are split into two subdomains. The (upper) part of the spherical domain in which the cylinder is located is assumed to be air, while the bottom part stands for the InP substrate.

For the cylinder representing the NW and for the substrate, material constants for InP were taken from Ref. 20. The meshing was done with the program built-in algorithm, which creates a tetrahedral mesh. The mesh maximum element size (MES), which limits the maximum size of the edges of the tetrahedrons, was set to be 20 nm in the domain representing the wire, 60 nm in the one representing the substrate, and 80 nm for all the elements in the air subdomains. The maximum element growth rate was set to 1.35 in all domains. Direct PARDISO solver was used in the simulations, indeed highly memory demanding (typically more than 150 GB) and time consuming, depending on the nanowire particular length.

ACKNOWLEDGMENTS

REFERENCES

1. J. Wang, M. S. Gudiksen, X. Duan, Y. Cui, and C. M. Lieber, "Highly polarized photoluminescence and photodetection from single indium phosphide nanowires," *Science (New York, N.Y.)* **293**, pp. 1455–7, Aug. 2001.
2. R. Yan, D. Gargas, and P. Yang, "Nanowire Photonics," *Nature Photonics* **3**, pp. 569–576, Oct. 2009.
3. D. Vanmaekelbergh and L. K. van Vugt, "ZnO nanowire lasers," *Nanoscale* **3**, pp. 2783–2800, July 2011.
4. A. V. Maslov and C. Z. Ning, "Reflection of guided modes in a semiconductor nanowire laser," *Applied Physics Letters* **83**(6), p. 1237, 2003.
5. O. L. Muskens, J. Gómez Rivas, R. E. Algra, E. P. A. M. Bakkers, and A. Lagendijk, "Design of Light Scattering in Nanowire Materials for Photovoltaic Applications," *Nano Letters* **8**(9), pp. 2638–2642, 2008.

6. S. L. Diedenhofen, G. Vecchi, R. E. Algra, A. Hartsuiker, O. L. Muskens, G. Immink, E. P. A. M. Bakkers, W. L. Vos, and J. Gómez Rivas, "Broad-band and Omnidirectional Antireflection Coatings Based on Semi-conductor Nanorods," *Advanced Materials* **21**, pp. 973–978, Mar. 2009.

7. L. Cao, J. S. White, J.-S. Park, J. A. Schuller, B. M. Clemens, and M. L. Brongersma, "Engineering light absorption in semiconductor nanowire devices," *Nature Materials* **8**, pp. 643–7, Aug. 2009.

8. J. Claudon, J. Bleuse, N. S. Malik, M. Bazin, N. Gregersen, C. Sauvan, P. Lalanne, and J.-M. Gerard, "A highly efficient single-photon source based on a quantum dot in a photonic nanowire," *Nature Photonics* **4**(March), pp. 174–177, 2010.

9. T. M. Babinec, B. J. M. Hausmann, M. Khan, Y. Zhang, J. R. Maze, P. R. Hemmer, and M. Loncar, "A diamond nanowire single-photon source," *Nature Nanotechnology* **5**, pp. 195–9, Mar. 2010.

10. T. Ba Hoang, A. F. Moses, L. Ahtapodov, H. Zhou, D. L. Dheeraj, A. T. J. van Helvoort, B.-O. Fim-land, and H. Weman, "Engineering parallel and perpendicular polarized photoluminescence from a single semiconductor nanowire by crystal phase control," *Nano Letters* **10**, pp. 2927–33, Aug. 2010.

11. K. Seo, M. Wober, P. Steinvurzel, E. Schonbrun, Y. Dan, T. Ellenbogen, and K. B. Crozier, "Multicolored vertical silicon nanowires," *Nano Letters* **11**, pp. 1851–6, Apr. 2011.

12. S. L. Diedenhofen, O. T. A. Janssen, M. Hocevar, A. Pierret, E. P. A. M. Bakkers, H. P. Urbach, and J. G. Rivas, "Controlling the Directional Emission of Light by Periodic Arrays of Hetero-structured Semiconductor Nanowires," *ACS Nano* **5**(7), pp. 5830–5837, 2011.

13. M. E. Reimer, G. Bulgarini, N. Akopian, M. Hocevar, M. B. Bavinck, M. A. Verheijen, E. P. A. M. Bakkers, L. P. Kouwenhoven, and V. Zwiller, "Bright single-photon sources in bottom-up tailored nanowires," *Nature Communications* **3**, p. 737, Jan. 2012.

14. G. Grzela, R. Paniagua-Domínguez, T. Barten, Y. Fontana, J. A. Sánchez-Gil, and J. Gómez Rivas, "Nanowire Antenna Emission," *Nano Letters* **12**, pp. 5481–5486, Oct. 2012.

15. J. Arnbak, "Leaky waves on a dielectric rod," *Electronics Letters* **5**(3), pp. 41–42, 1969.

16. A. V. Maslov and C. Z. Ning, "Far-field emission of a semiconductor nanowire laser," *Optics Letters* **29**, pp. 572–4, Mar. 2004.

17. H. Ruda and A. Shik, "Polarization-sensitive optical phenomena in semiconducting and metallic nanowires," *Physical Review B* **72**, pp. 1–11, Sept. 2005.

18. H. E. Ruda and A. Shik, "Polarization-sensitive optical phenomena in thick semiconducting nanowires," *Journal of Applied Physics* **100**(2), p. 024314, 2006.

19. I. Friedler, C. Sauvan, J. P. Hugonin, P. Lalanne, J. Claudon, and J. M. Gérard, "Solid-state single photon sources: the nanowire antenna," *Optics Express* **17**, pp. 2095–110, Mar. 2009.

20. E. D. Palik, *Handbook of Optical Constants of Solids*, vol. 3, Academic Press, 1998.